Arsenite Causes DNA Damage in Keratinocytes Via Generation of Hydroxyl Radicals

Honglian Shi,[†] Laurie G. Hudson,[†] Wei Ding,[†] Suwei Wang,[‡] Karen L. Cooper,[†] Shimin Liu,[†] Yan Chen,[§] Xianglin Shi,[‡] and Ke Jian Liu*,[†]

Program in Toxicology, College of Pharmacy, University of New Mexico Health Sciences Center, Albuquerque, New Mexico 87131, Pathology and Physiology Research Branch, National Institute for Occupational Safety and Health, Morgantown, West Virginia 26505, and Department of Medical and Molecular Genetics, Indiana University School of Medicine, Indianapolis, Indiana 46202

Received February 20, 2004

Arsenic is an environmental and occupational toxin. Dermatologic toxicities due to arsenic exposure are well-documented and include basal cell and squamous cell carcinomas. However, the mechanism of arsenic-induced skin cancer is not well-understood. Recent studies indicate that arsenic exposure results in the generation of reactive oxygen species (ROS) and oxidative stress. Here, we examined the chemical nature of the specific ROS, studied the interrelationship among these species, and identified the specific species that is responsible for the subsequent DNA damage in a spontaneously immortalized keratinocyte cell line. We detected the formation of $O_2^{\bullet-}$ and H_2O_2 in keratinocytes incubated with arsenite [As(III)] but not with arsenate. As(III)-induced DNA damage was detected in a concentration-dependent manner and evident at low micromolar concentrations. Catalase, an H_2O_2 scavenger, eliminated H_2O_2 and reduced the As(III)-mediated DNA damage. Superoxide dismutase, by enhancing the production of H_2O_2 and $^{\bullet}OH$, significantly increased the As(III)-mediated DNA damage. Sodium formate, a competitive scavenger for $^{\bullet}OH$, and deferoxamine, a metal chelator, both reduced the DNA damage. These results suggest that exposure to arsenite generates $O_2^{\bullet-}$ and H_2O_2, and $^{\bullet}OH$, derived from H_2O_2, is responsible, at least in part, for the observed DNA damage. These findings demonstrate arsenic-induced formation of specific ROS and provide the direct evidence of $^{\bullet}OH$-mediated DNA damage in keratinocytes, which may play an important role in the mechanism for arsenic-induced skin carcinogenicity.

Introduction

As[1] is a naturally occurring element that is present in food, soil, and water. Environmental or occupational exposures to As may result in both acute and chronic toxic effects in humans. Epidemiological studies have indicated that people exposed to high levels of As are prone to develop skin, bladder, liver, and lung cancers (*1*). In addition to its carcinogenic effects, As exposure has been suggested to play a role in black foot disease, type II diabetes mellitus, and cardiovascular diseases (*2*−*4*).

The skin is one identified target tissue for As toxicity. Organic and inorganic As can be absorbed through the skin by animals and humans (*5*). As accumulates in the skin and is associated with hyperkeratosis and acanthosis, pigmentation disorders, and keratinocytic tumors including basal cell carcinoma and squamous cell carcinoma. Occupational or medical exposure to As has caused many cases of skin cancer (*5*), and although As has been identified as a complete carcinogen, the cellular and molecular carcinogenic mechanisms are still not known.

As exposure leads to various types of DNA damage. As has been reported to promote chromosomal aberrations and sister chromatid exchange and induce DNA hyper- and hypomethylation (*6*−*8*). As interferes with DNA methyltransferases, resulting in inactivation of tumor suppressor genes through DNA hypermethylation. Other studies suggest that As-induced malignant transformation is linked to DNA hypomethylation after the depletion of S-adenosyl-methionine, which results in aberrant gene activation, including oncogenes (*9*). It has also been proposed that genetic damage induced by exposure to As may be due in part to the inhibition of DNA repair (*10*).

Another potential mechanism for As-induced DNA damage is the generation of ROS (*11*). ROS generation by metals is associated with a range of DNA damage including double strand and single strand DNA breaks (*12*, *13*), the induction of DNA−protein cross-links (*14*), hydroxylation of 2′-deoxyguanosine (*15*), and deletion mutations (*16*). ROS refers to a diverse group of reactive, short-lived, oxygen-containing species, such as $O_2^{\bullet-}$, H_2O_2, $^{\bullet}OH$, singlet oxygen ($^1O_2$), etc. The generation of several specific as well as nonspecific ROS species has been reported in various cellular systems exposed to As at various concentrations (*13*, *17*−*22*). For example, in endothelial cells, superoxide and H_2O_2 were produced

* To whom correspondence should be addressed. Tel: 505-272-9546. Fax: 505-272-6749. E-mail: jliu@unm.edu.
[†] University of New Mexico Health Sciences Center.
[‡] National Institute for Occupational Safety and Health.
[§] Indiana University School of Medicine.

[1] Abbreviations: As, arsenic; As(III), arsenite; As(V), arsenate; DCFH-DA, 2′,7′-dichlorofluorescein diacetate; DHE, dihydroethidium; HaCat, human keratinocyte cell line; H_2O_2, hydrogen peroxide; $O_2^{\bullet-}$, superoxide anion; $^{\bullet}OH$, hydroxyl radical; ROS, reactive oxygen species; SCG, single cell gel electrophoresis; SOD, superoxide dismutase.

10.1021/tx049939e CCC: $27.50
Published on Web 06/24/2004

after As(III) exposures and the consumption of oxygen in these cells was significantly increased (*23*). These various reports establish the fact that the exposure of diverse cellular systems to As generates ROS. However, these isolated and scattered results have not been able to provide a clear overall view of what exact specific ROS species are generated, as the various and distinctly different reactive species have a complex intricate relationship. More importantly, it is not clear what specific species are involved in, and responsible for, the observed As toxicity and carcinogenesis. Furthermore, despite evidence that skin is a target issue for As toxicity, there are no published studies to directly evaluate the generation of specific ROS in keratinocytes following exposure to As.

We hypothesized that ROS and DNA damage play an important role in As-induced skin cancer, and we examined ROS generation and subsequent DNA damage in a spontaneously immortalized keratinocyte cell line. In the present study, we find that inorganic As induces ROS generation in human keratinocytes, the ROS species generated in this system include superoxide and H_2O_2, and As-mediated DNA damage is mediated by $^{\bullet}OH$. These findings expand our understanding of the potential mechanisms underlying As-mediated skin carcinogenesis.

Materials and Methods

Materials. Sodium As(III), sodium formate, deferoxamine, SOD, catalase, DHE, DCFH-DA, and cell culture reagents were purchased from Sigma (St. Louis, MO) unless otherwise noted. All of the chemicals were the highest grade available.

Cell Culture and Treatment. HaCat was generously provided by Dr. Mitch Denning (Loyola University Medical Center, Maywood, IL). HaCat cells were maintained in Dulbecco's modified Eagle's medium F:12 HAM (DMEM F:12), supplemented with 10% newborn calf serum from Life Technologies/Gibco, a 4-fold concentration of Eagle's minimal essential medium (MEM) Amino Acids Solution, 2 mM L-glutamine, and antibiotics (penicillin, 100 U/mL, and streptomycin, 50 μg/mL). The cells were cultured at 37 °C in 95% air/5% CO_2 humidified incubators. For all experiments involving stimulation with As, HaCat cells were rinsed in PBS and placed into DMEM F:12 containing 0.1% bovine serum albumin for 24 h prior to As(III) addition. Antioxidants, sodium formate, and deferoxamine were dissolved in PBS and added 30 min prior to As(III) exposure.

The mouse keratinocyte cell line JB6 was cultured in a monolayer in MEM containing 5% fetal bovine serum, 2 mM L-glutamine, and 25 μg gentamicin/mL. The fetal bovine serum was from Life Technologies, Inc. (Rockville, MD) (*26*). The MEM was from Calbiochem (San Diego, CA).

Cellular $O_2^{\bullet-}$ Assay. DHE was dissolved in DMSO to a final concentration of 2 mM and kept at −20 °C in a foil-wrapped container. The HaCat cells were plated onto glass cover slips in eight well plates and cultured to 50−60% confluence. After the cells were washed with PBS three times, the medium was changed to DMEM (without the serum and amino acids). DHE was added to the cell culture concomitantly with the various treatments, and the plates were wrapped with foil to avoid light and incubated at 37 °C for 30 min. The final DMSO concentration in the cell culture was 0.2%. The stained cells were then washed with PBS and fixed with 4% paraformaldehyde at room temperature for 5 min. The cover slips were mounted on a glass slide using Gel/Mount (Biomedia Corp., Foster City, CA). An Olympus BH2-RFCA fluorescence microscope (Olympus Optical Co., Tokyo, Japan) and a laser scanning confocal microscope (Optiphot-2, Nikon, Inc., Melville, PA) fitted with an argon ion laser were used for imaging.

H_2O_2 Detection by Flow Cytometry. HaCat cells were seeded into six well plates at 1.0×10^5 cells and cultured to 80% confluence. The cells were detached with trypsin and suspended in media at 2.0×10^5/mL. The cells were incubated with DCFH-DA (20 μM) in the presence of various concentrations of As(III) at 37 °C for 15 min. Catalase (10 000 U/mL) was added to the samples 1 h before the addition of 50 μM As(III). The cells were washed twice with PBS and put on ice until flow cytometry measurement (FACScan, Becton Dickinson). The results are expressed as the mean channel fluorescence of 10 000 gated events and corrected for background fluorescence.

SCG Assay for DNA Damage. The cells (2.5×10^6) were seeded in 35 mm cell culture plates and incubated overnight. The cells were exposed to different concentrations of As(III). After incubation, the cells were harvested and resuspended in the PBS at an approximate density of 2×10^6 cells/mL for the SCG assay. The SCG assay was performed according to the procedure described by Tice et al. (*24*). Briefly, 100 μL of 0.5% normal melting agarose (Sigma) in Ca^{2+} and Mg^{2+} free PBS was added onto the fully frosted microscope slides. The agarose was immediately covered with a 22 mm × 22 mm coverslip, and the slides were placed on ice for 10 min. A 100 μL cell suspension was mixed with 900 μL low melting point (LMP) agarose at 37 °C, and 75 μL of the mixture (approximate $1.5-2.0 \times 10^4$ cells) was pipetted onto the first agarose layer (after the coverslip was gently removed). The coverslip was replaced, and the slide was maintained at 4 °C for solidification. After the coverslip was removed, 75 μL of 0.5% LMP agarose was loaded. The coverslip was replaced, and the gel was allowed to solidify for 10 min. The coverslip was removed, and the slides were immersed in freshly prepared cold lysing solution (2.5 M NaCl, 100 mM Na_2-EDTA, 10 mM Tris, and 1% sodium sarcosinate, pH 10, 1% Triton X-100, and 10% DMSO v/v) for at least 1 h at 4 °C. All of the following steps were conducted under red light to prevent additional DNA damage. The slides were drained and placed in a horizontal gel electrophoresis tray filled with fresh alkaline EDTA buffer (300 mM NaOH and 1 mM EDTA in distilled water, pH > 13) for 10 min to allow for DNA unwinding and alkaline labile damage expression. Electrophoresis was carried out for 50 min at room temperature at 20 V (about 1 V/cm). Then, the slides were neutralized by rinsing three times for 5 min each with Tris buffer (0.4 M Tris, pH 7.5), stained with 50 μL of ethidium bromide (20 μg/mL), and covered with a coverslip. Image analysis was conducted at 400× magnification using a fluorescence microscope (Zeiss). The length of DNA migration was determined by measuring the tail length (distance between the edge of head and the end of tail) with an optical micrometer. A minimum of 50 cells per treatment from a randomly chosen field was scored.

Statistical Analysis. Each experiment was performed a minimum of three times. The data are graphed as means ± SD. Statistical significance analysis was performed by using Student's *t*-test.

Results

As(III)-Mediated DNA Damage in Keratinocytes. The functional impact of ROS generation was investigated by measurement of As-induced DNA damage in the murine keratinocyte line JB6. Other ROS-generating metals such as chromium cause DNA strand breaks, as our recent study has shown (*25*). The mouse keratinocyte line JB6 was selected because ROS-dependent DNA damage by chromium is well-documented in this model (*25*−*29*). As-induced DNA damage was detected within 4 h in a concentration-dependent manner with statistically significant differences evident at 10 μM As(III) (Figure 1A). Upon extended As exposure for 24 h, DNA damage was apparent at As(III) concentrations as low as 1.25 μM (Figure 1B). The level of DNA damage was similar between incubation with 10 μM As(III) for 4 h and incubation with 1.25 μM As(III) for 24 h. In addition, the overall trend of DNA damage at low As(III) concen-

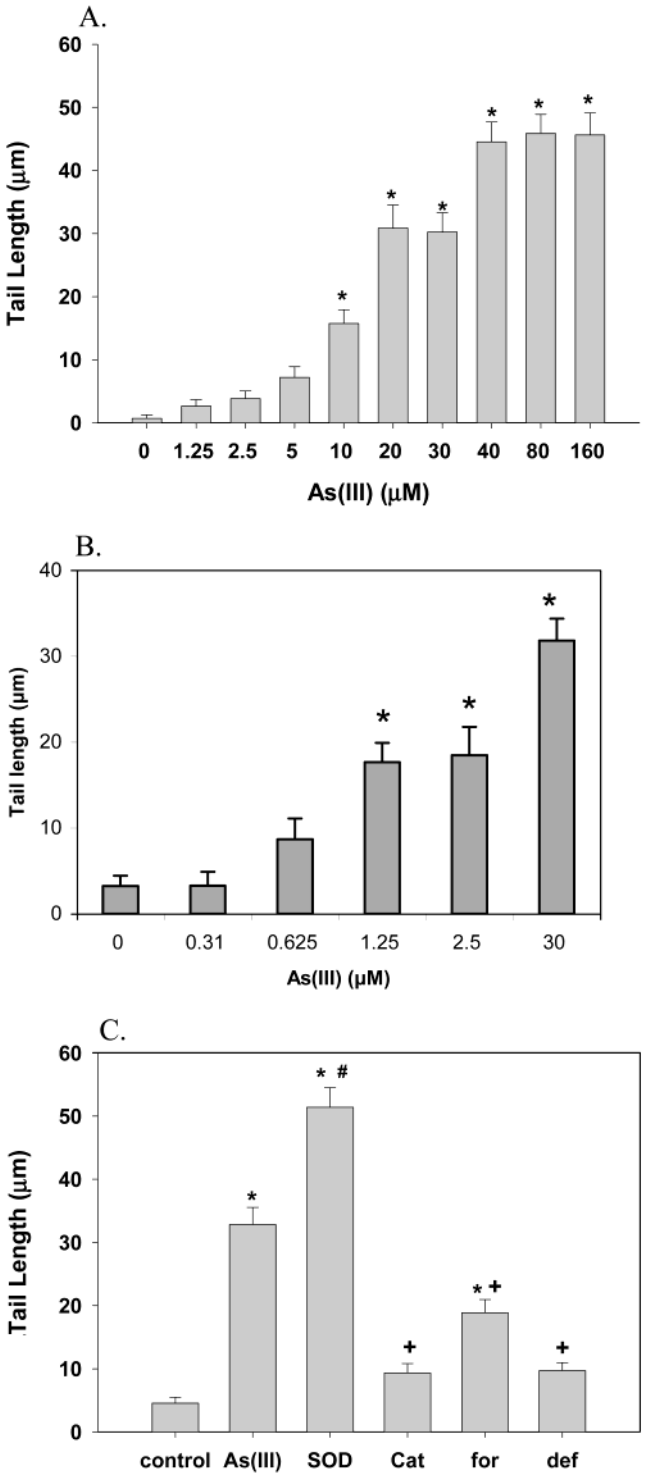

Figure 1. As(III)-induced cellular DNA damage in murine ketatinocyte JB6 cells. (A) Cells were incubated for 4 h with the indicated concentrations of As(III) and then harvested and resuspended in PBS. DNA damage was determined by the SCG assay (comet assay). The asterisk indicates a significant increase from the control ($p < 0.05$). (B) Cells were treated for 24 h with the indicated concentrations of As(III), and DNA damage was assessed as described in A above. (C) Cells were pretreated with the indicated antioxidants for 30 min prior to 3 h of incubation with As(III), and DNA damage was assessed as described above. Control, no treatment; As(III), 20 μM As(III); SOD, 20 μM As(III) + 500 units/mL SOD; Cat, 20 μM As(III) + 10 000 unit/mL catalase; For, 20 μM As(III) + 50 mM sodium formate; Def, 20 μM As(III) + 2 mM deferoxamine.

trations with extended incubation times (Figure 1A) vs high concentrations with short incubation times (Figure 1B) is also very similar. These results suggest that the effect on DNA damage is a product of exposure time and As concentration and that the mechanism of the observed DNA damage at 10 μM As(III) is highly likely to be the same with 1.25 μM As(III). Therefore, we used relatively high concentrations of 10 μM and above with short exposure times (1 h or less) to study the generation of ROS in the following experiments, which is to overcome the limitation of detection by the currently available methods.

The addition of SOD, a superoxide scavenger that converts superoxide to H_2O_2, significantly increased DNA strand breaks (Figure 1C) as expected if $^{\bullet}$OH is the major DNA damaging species. Supporting evidence that $^{\bullet}$OH formation is involved in As(III)-stimulated DNA damage is provided by protection from DNA strand breaks when cells were cotreated with catalase, a H_2O_2 scavenger, sodium formate, a scavenger of $^{\bullet}$OH, and deferoxamine, a metal chelator (Figure 1C). These results indicate that $^{\bullet}$OH formation is involved in the observed DNA damage and demonstrate that free radicals generated by As can cause DNA damage in keratinocytes.

Generation of $O_2^{\bullet-}$ by As in Keratinocytes. We hypothesized that superoxide represents the parent (primary) species in As-stimulated ROS production and that superoxide is responsible for the subsequent formation of other reactive species. DHE is a specific molecular probe for superoxide detection that when oxidized by superoxide intracellularly, stains the nucleus a bright fluorescent red, which can be observed by fluorescence microscopy (*30*). As shown in Figure 2, superoxide is generated when HaCat cells are treated with trivalent As(III), as detected by the increased fluorescence intensity (Figure 2E,F). In the presence of SOD (Figure 2H) or a membrane permeable SOD mimic (MnTMpyP) (Figure 2G), the metal-induced increase in fluorescence intensity was completely abolished, confirming the generation of superoxide under these conditions. To validate the method, we also used chromium, another carcinogenic metal ion known to generate superoxide (*25*), as a positive control. Figure 2B shows that incubation of HaCat cells with chromium generated superoxide, while the addition of SOD or SOD mimic MnTMpyP returned the fluorescence intensity to the level of control (Figure 2C,D).

The response to As was concentration-dependent with an increase in superoxide production evident following exposure to 10 μM As(III) for 30 min (Figure 3). Furthermore, superoxide generation could be detected as early as 5 min after exposure and the response continued to increase with additional incubation time (Figure 4). In contrast, the treatment of HaCat cells with pentavalent As(V) does not produce a detectable increase of fluorescence intensity from the control, even at the significantly higher concentration of 100 μM (Figure 5). Because trivalent As(III) is more toxic than pentavalent As(V), this result is consistent with a relationship between ROS-generating capacity and resulting toxicity.

The above results were obtained in human keratinocytes with regular fluorescence microscopy. To further confirm the generation of superoxide, we used confocal microscopy to monitor simultaneously the disappearance of the DHE itself and the appearance of the oxidized product in the presence of As in a murine keratinocyte cell line, JB6. There are three columns in Figure 6: column A shows the red channel to monitor the fluorescence from the product of DHE oxidized by superoxide

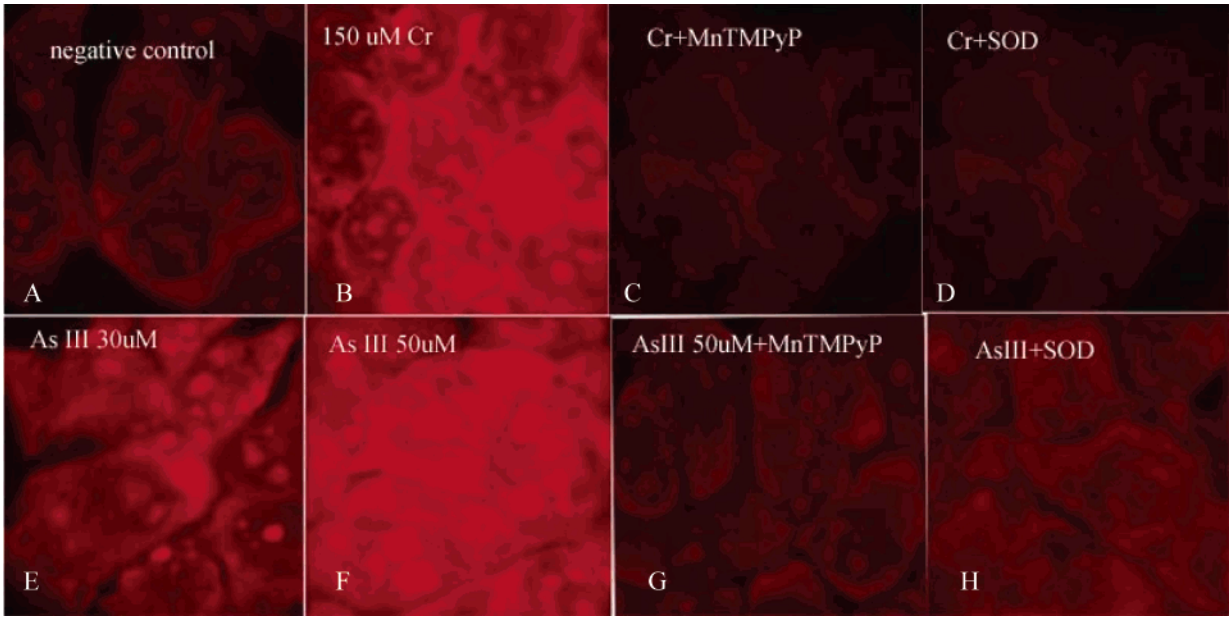

Figure 2. As-stimulated superoxide generation in HaCat cells. Top row: HaCat cells incubated with 2 μM DHE at 37 °C for 30 min in the absence of As was used as a negative control (A) and HaCat cells incubated with 2 μM DHE in the presence of 150 μM sodium dichromate as a positive control (B). After the addition of 2 μM MnTMpyP (C) or 1000 U/mL SOD (D), the fluorescence intensity returned to the control level. Bottom row: Incubation with 30 (E) or 50 μM (F) sodium As(III) increased the fluorescence intensity, while this increase was abolished when 2 μM MnTMpyP (G) or 1000 U/mL SOD (H) was added into the incubation.

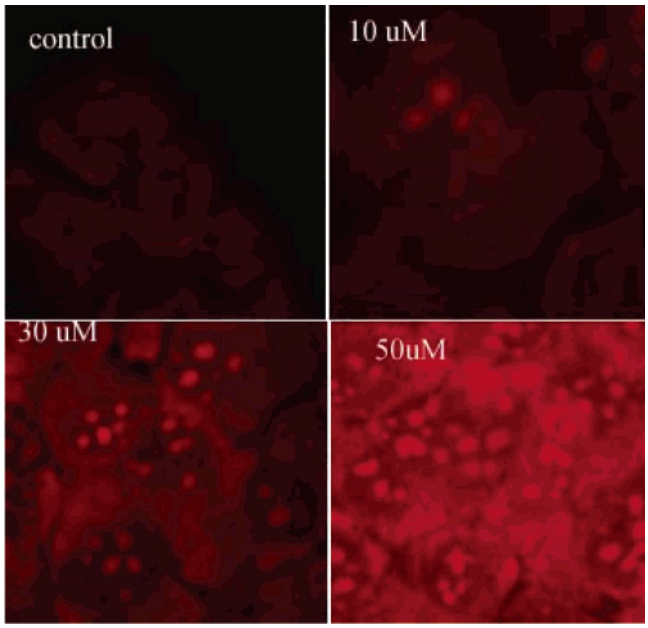

Figure 3. Concentration-dependent superoxide generation in HaCat cells by As. The cells were incubated with DHE (2 μM) in the absence or presence of 10, 30, or 50 μM sodium As(III) at 37 °C for 30 min. Then, the cells were washed once in PBS and fixed with 10% buffered formalin. The treatment of the cells with As(III) dramatically enhanced the fluorescence intensity as compared to the control (cells + DHE only), suggesting the production of superoxide.

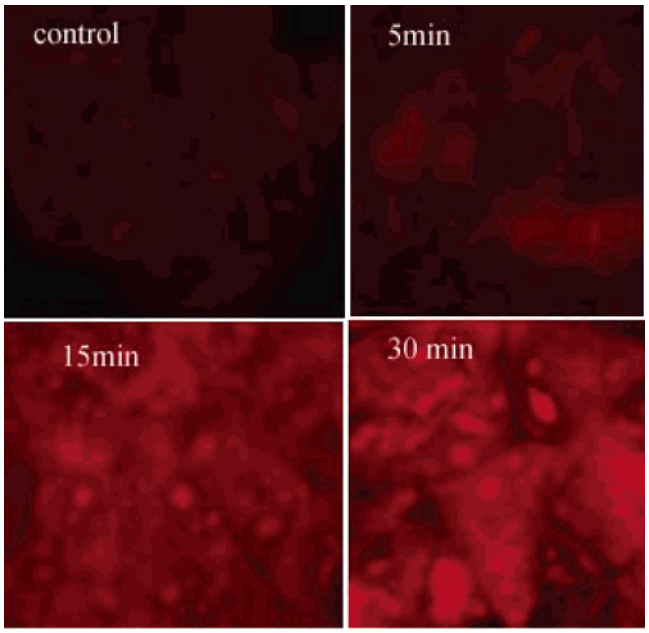

Figure 4. Time-dependent superoxide generation in HaCat cells by As. HaCat cells were incubated with 30 μM sodium As(III) in the presence of 2 μM DHE for 0, 5, 15, or 30 min. Then, the cells were washed once in PBS, fixed with 10% buffered formalin, and observed under fluorescence microscopy. The fluorescence intensity increased with incubation time.

(*30*), therefore indicating the generation of superoxide; column B shows the blue channel to monitor the fluorescence of DHE itself before its conversion to the red-colored oxidized form by superoxide; and column C shows the combined blue and red channels. As shown in the first row of Figure 6, fluorescence was only observed in the blue channel in control cells [in the absence of As(III)] indicating the existence of DHE and the absence of DHE oxidation. With As(III)-treated cells (second row), fluorescence was observed in the red channel and only weak fluorescence appeared in the blue channel indicating that a significant amount of DHE had been converted into the oxidized form, which suggests that As(III) indeed caused the generation of superoxide. The addition of SOD, a scavenger of superoxide, blocked the oxidation of DHE (third row). Therefore, the cells remained blue (column B) and the red color did not appear (column A), confirming that superoxide was indeed produced in the cells exposed to As(III), which was responsible for the conversion of DHE to the oxidized form by superoxide, and this conversion could be blocked by SOD. Together,

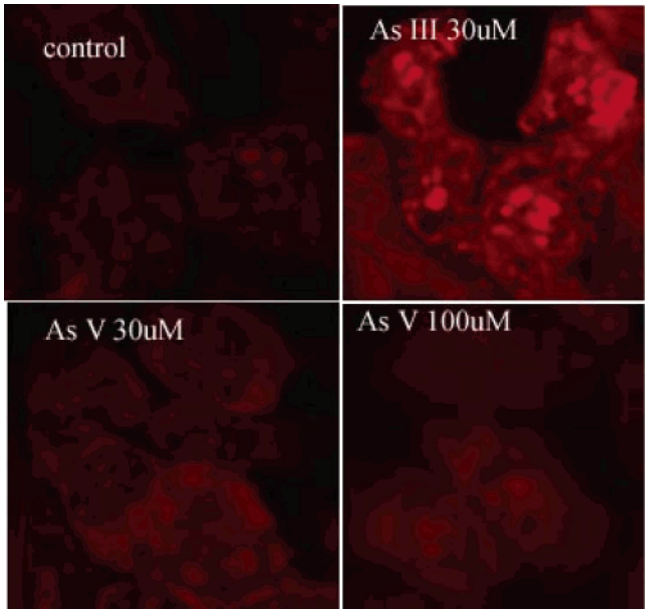

Figure 5. Comparison of superoxide generation by different As compounds. HaCat cells were incubated with 30 μM As(III) and 30 and 100 μM As(V) in the presence of 2 μM DHE or 2 μM DHE alone (control) at 37 °C for 20 min. Then, the cells were washed once in PBS, fixed with 10% buffered formalin, and observed under fluorescence microscopy.

these findings demonstrate that As(III) stimulates superoxide production in keratinocytes in a concentration- and time-dependent manner.

Generation of H_2O_2 Anion by As in Keratinocytes. To further understand free radical generation pathways induced by As(III) in keratinocytes, DCFH-DA, a specific fluorescent molecular probe for H_2O_2 (*31*, *32*), was used to detect intracellular H_2O_2. As shown in Figure 7, As(III) exposure increased H_2O_2 production significantly at the concentration of 5 μM within 15 min of incubation. The production of H_2O_2 in HaCat cells was As(III) concentration-dependent in the test concentration range, 0−100 μM. Catalase (10 000 U/mL) completely blocked H_2O_2 production in cells incubated with 50 μM As(III). The results indicate that As(III) stimulates H_2O_2 generation in HaCat cells.

Discussion

ROS have been implicated as an underlying mechanism in As-induced toxicity and carcinogenesis. Experimental results show that As can induce $O_2^{\bullet-}$ and H_2O_2 generation in various cellular systems. As(III) generates detectable levels of $O_2^{\bullet-}$ in U937 cells at the concentration of 1−10 μM (*33*), human vascular smooth muscle cells (VSMC) at 7−16 μM (*34*), and human−hamster hybrid cells at 50 μM (*18*). At environmentally relevant concentrations or at nonlethal concentrations (below 5 μM), As could also stimulate $O_2^{\bullet-}$ and H_2O_2 formation in vascular endothelial cells (*23*). Moreover, H_2O_2 has been reported to be involved in transcription factor Nrf2 activation by inorganic As in cultured keratinocytes HaCat (*35*). The induction of H_2O_2 has been found in other cell types exposed to As. In HEL30 cells, As(III) (1−50 μM) elevated the levels of H_2O_2 as measured by the oxidation of DCFH (*20*). The production of H_2O_2 appears to be involved in the induction of apoptosis by As(III) in NB4 cells (*36*) and Chinese hamster ovary (CHO)-K1 cells (*37*). H_2O_2 resistant CHO cells are also cross-resistant to As(III) (*22*). It has been suggested that As(III)-induced apoptosis in CHO-K1 cells was initiated by the production of $^{\bullet}OH$, which selectively activates protein kinase through de novo synthesis of macromolecules (*37*). However, the effect of As on the generation of ROS in skin cells, a sensitive and important target of As, has not been systematically studied. In the present study, we investigated the effects of As(III) on ROS generation in HaCat cells induced by As(III). The results show that exposure of HaCat cells to As(III) leads to an increase in superoxide production as observed by fluorescence microscopy and laser microscopy and confirmed by the effect of the addition of SOD. We also found that the level of H_2O_2 in the HaCat cells increased significantly in the presence of As(III). Furthermore, we found that As caused DNA damage in keratinocytes with $^{\bullet}OH$ involvement. Importantly, DNA damage could be detected at environmentally relevant As concentrations (<5 μM). There results demonstrated that As(III) could induce the generation of ROS and DNA damage in keratinocytes.

There is an interrelationship among the distinctively different ROS, $O_2^{\bullet-}$, H_2O_2, and $^{\bullet}OH$. Although many studies including the above-mentioned reports have identified As-induced free radical generation, the free radical pathway has not been elaborated. From our findings, we suggest an overall As-stimulated free radical pathway in keratinocytes (Figure 8). The generation of $O_2^{\bullet-}$ following As(III) exposure can be regarded as a primary species that gives rise to H_2O_2 and oxygen through catalysis by SOD. H_2O_2 can be converted in a spontaneous reaction catalyzed by Fe^{2+} (Fenton reaction) to the highly reactive $^{\bullet}OH$. Importantly, our results indicated that $^{\bullet}OH$ is involved in the observed As(III)-dependent DNA damage. The addition of a $^{\bullet}OH$ scavenger (sodium formate) and a metal chelator (deferoxamine) that prevents the production of $^{\bullet}OH$ from H_2O_2 significantly inhibited DNA damage caused by As (Figure 1C). Furthermore, while catalase almost totally abolished the DNA damage, the addition of SOD actually enhanced As-induced DNA damage. The latter would be expected because the addition of SOD will generate more H_2O_2 through superoxide dismutation and, hence, give rise to a greater production of $^{\bullet}OH$.

ROS play an important role in carcinogenesis (*38*). Unregulated or prolonged production of cellular oxidants has been linked to mutation (induced by oxidant-induced DNA damage), as well as modification of gene expression. Evidence from DNA microarray studies shows large perturbations of gene transcription in normal and neoplastic human keratinocytes treated with As(III), and ROS are regarded as a cause of the perturbations of gene transcription (*39*). Inhibition of methylation of DNA (*8*) and large deletional mutations of DNA (*16*) contribute to carcinogenic effects of As exposure. DNA strand breakage is an important form of DNA damage. DNA single strand breakage is an obligatory trigger for the activation of poly (ADP-ribose) polymerase (PARP), which can result in the consumption of NAD, the depletion of ATP, and cell death. PARP also plays a role in DNA replication, DNA repair, gene expression, and carcinogenesis (*40*). DNA strand breaks can also cause chromosomal rearrangements. As(III)-induced DNA strand breaks have been observed in human fibroblast cells (*41*), human VSMCs (*13*), human leukemia cells, and CHO cells (*42*). Our results clearly show that As(III) induces DNA strand breaks in keratinocytes (Figure 1), and the DNA damage

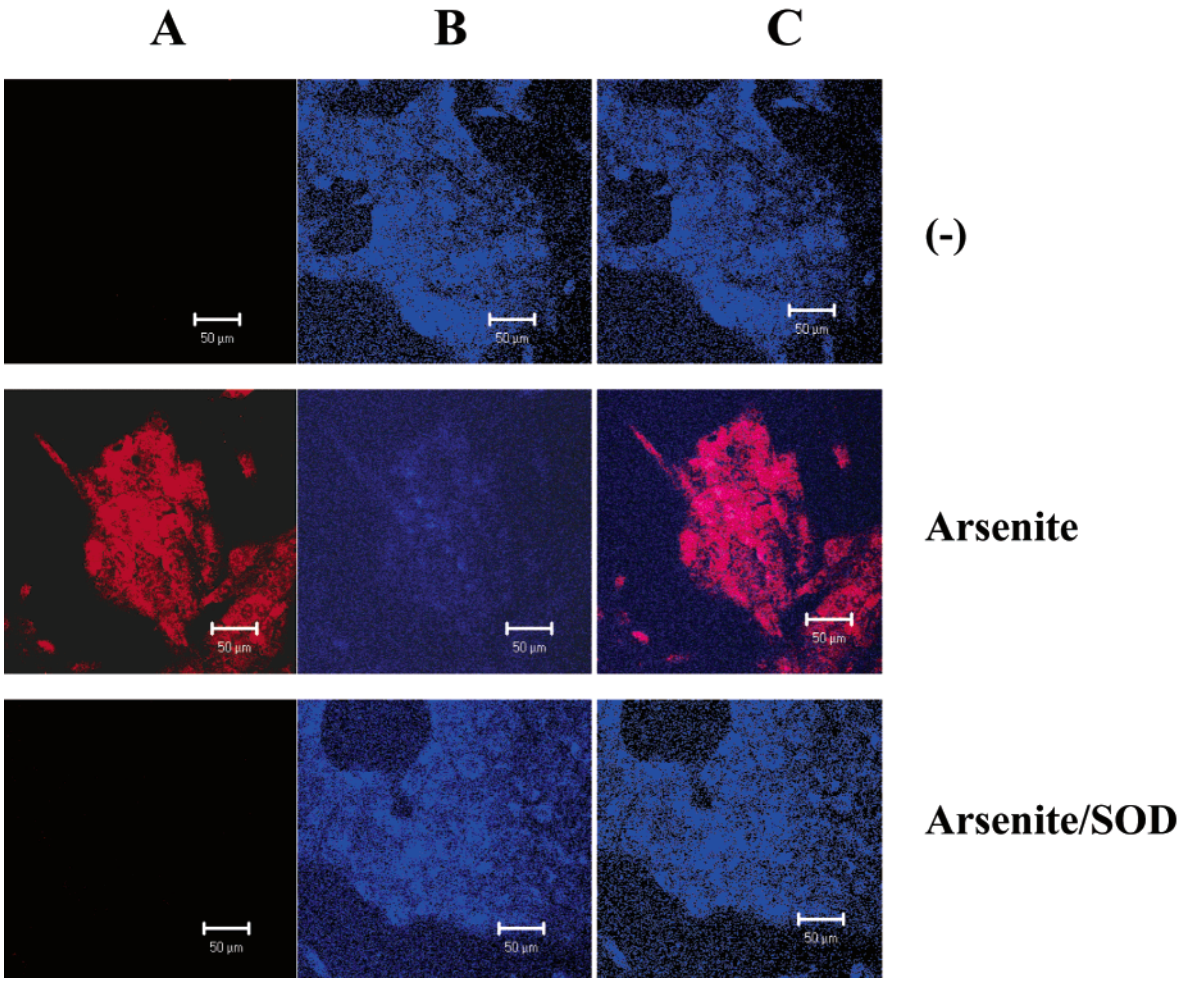

Figure 6. Generation of superoxide in murine keratinocytes detected by confocal microscopy. JB6 cells were cultured in a six well plate. After they reached 80−90% confluence, the cells were treated with 100 μM As(III) for 1 h. For the evaluation of antioxidant effects, the cells were pretreated with 500 U/mL SOD for 0.5 h before treatment with 100 μM As(III). DHE was added to the cells and incubated for another 15−20 min at 37 °C. Then, the cells were washed with PBS twice and analyzed using confocal microscopy. Column A, red channel to monitor the fluorescence of the oxidized form of DHE by superoxide; column B, blue channel to monitor the fluorescence of DHE itself; and column C, combined blue and red channels.

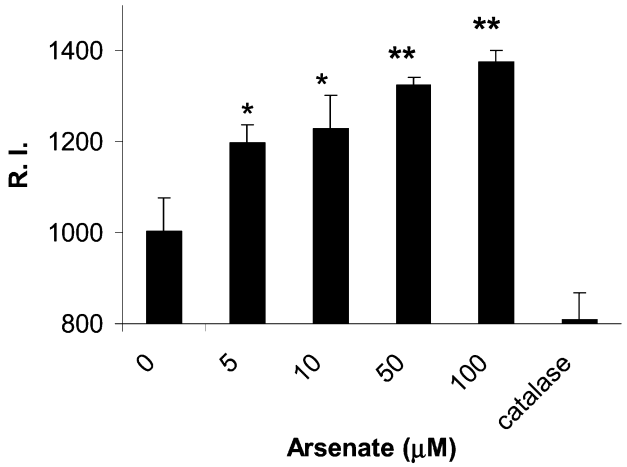

Figure 7. H_2O_2 generation in HaCat cells induced by As(III). The cells (2.0×10^5/cells) were incubated with DCFH-DA (20 μM) in the presence of various concentrations of As(III) at 37 °C for 15 min. The cells were washed twice with PBS and placed on ice until flow cytometry measurement. Catalase (10 000 units/mL) was added to the samples with 50 μM As(III); RI, relative intensity. The data were expressed as means ± SD; $n = 3-5$. *$p < 0.5$; **$p < 0.01$ vs As(III) at 0 μM.

is As(III) concentration-dependent. Increased exposure times require lower concentrations of As(III). As at 10 μM induced statistically significant DNA strand breaks for 4 h of incubation while 1.25 μM As did so when the incubation time was prolonged to 24 h. Although the limitations of current detection methods prevented us from measuring specific ROS generation at concentrations as low as 1.25 μM, it is highly possible that the DNA damage was caused by free radicals produced at smaller amounts as compared to those at higher As concentrations. The prolonged incubation maintained a continuous attack on DNA by the generated ROS, and accumulated damage was observed.

Several metals other than As are known carcinogens. It has been found that ROS are involved in metal-induced carcinogenesis. However, the mechanism of ROS generation induced by other metals may be different from that of As. For example, unlike As, which may produce ROS through the mitochondrial electron transfer chain, chromium has been mainly reported to produce ROS by its redox reaction (*27*, *43*−*45*). •OH appears to be one of the most significant species among chromium-generated free radicals in terms of causing DNA damage. Thus, there are differences in the mechanisms of free radical generation induced by different metals but similarities in the outcomes of ROS. This suggests that the generation of free radicals may be a shared mechanism of toxicity

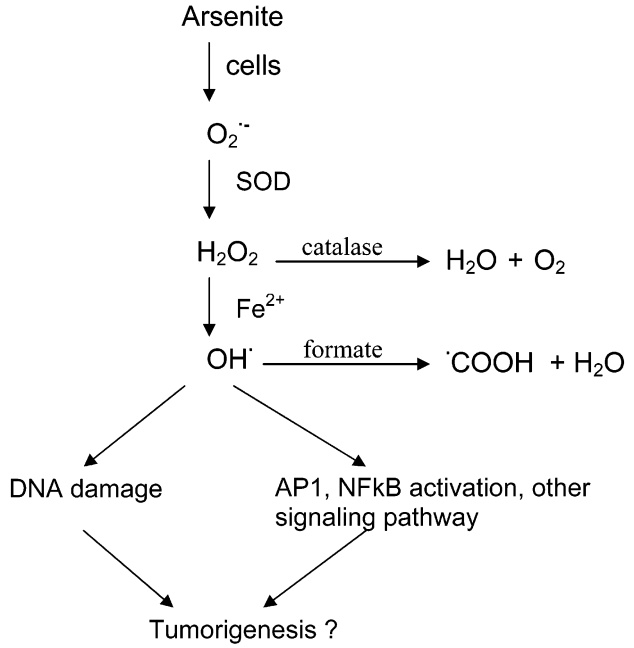

Figure 8. Schematic representation of the possible mechanism of the generation of various ROS and their roles in As-mediated carcinogenicity. The generation of $O_2^{\bullet-}$ following As(III) exposure is a primary or parent species that gives rise to H_2O_2 and oxygen through catalysis by SOD. H_2O_2 can be converted to the highly reactive $^{\bullet}OH$ leading to the observed As(III)-dependent DNA damage. Additionally, As may activate redox sensitive transcription factors such as NF-κB and AP-1 (*1*) that have been shown to play important roles in tumor promotion and skin carcinogenesis.

although the pathways leading to free radical generation differ between metals.

Our findings as well as other reports demonstrate that As exposure results in the generation of ROS in various cellular systems. However, the source or mechanism of the ROS formation remains unclear. Mitochondria have been suggested as one of the sources of ROS production. The increase in cellular ROS induced by As(III) could be completely abrogated by rotenone in HEL30 cells, indicating mitochondria as the intracellular source of ROS induced by As(III) (*20*). As(III) may increase free radical production at the ubiquinone site of the respiratory chain. Aside from mitochondria, there are several other proposed sources of ROS: the reaction between dimethylarsine and molecular oxygen (*46*−*48*), free iron released by methylated As species (*49*, *50*), and oxidation of As(III) to As(V) (*51*). Further studies are needed to identify the contributions of other sources of ROS. Despite the source of ROS generation, our results suggest that the superoxide is generated in cells (Figures 2−6).

Inducing DNA damage may only be one of the biological effects of free radicals generated in cells exposed to As. ROS, especially H_2O_2 and $^{\bullet}OH$, can activate NF-κB, AP-1, and p53 transcription factors, which play a role in carcinogenesis. As may induce activation of redox sensitive transcription factors such as NF-κB and AP-1 by ROS (*20*). AP-1 activation is required in the development of skin cancer (*52*). The scheme presented in Figure 8 is an illustration of possible pathways for ROS generation and carcinogenesis in skin exposed to As.

In summary, our findings indicate that As(III) exposure induces superoxide generation in keratinocytes, from which H_2O_2 and $^{\bullet}OH$ are subsequently produced. As(III) induces DNA damage, and the $^{\bullet}OH$ is a key player in the observed DNA damage. These findings demonstrate the As-induced formation of specific ROS and provide the direct evidence of $^{\bullet}OH$-mediated DNA damage in keratinocytes, which may play an important role in the mechanism for As-induced skin carcinogenicity.

Acknowledgment. This research was supported in part by grants from the NIH (R01 ES012938, R01 AR42989, P20 RR15636, and P30 ES012022) and American Heart Association (0040041N).

References

(1) Shi, H., Shi, X., and Liu, K. J. (2004) Oxidative mechanism of arsenic toxicity and carcinogenesis. *Mol. Cell. Biochem. 255*, 67−78.

(2) Engel, R. R., Hopenhayn-Rich, C., Receveur, O., and Smith, A. H. (1994) Vascular effects of chronic arsenic exposure: A review. *Epidemiol. Rev. 16*, 184−209.

(3) Tseng, C. H., Tai, T. Y., Chong, C. K., Tseng, C. P., Lai, M. S., Lin, B. J., Chiou, H. Y., Hsueh, Y. M., Hsu, K. H., and Chen, C. J. (2000) Long-term arsenic exposure and incidence of noninsulin-dependent diabetes mellitus: A cohort study in arseniasis-hyperendemic villages in Taiwan. *Environ. Health Perspect. 108*, 847−851.

(4) Tseng, C. H., Chong, C. K., Chen, C. J., and Tai, T. Y. (1996) Dose−response relationship between peripheral vascular disease and ingested inorganic arsenic among residents in blackfoot disease endemic villages in Taiwan. *Atherosclerosis 120*, 125−133.

(5) Lansdown, A. B. (1995) Physiological and toxicological changes in the skin resulting from the action and interaction of metal ions. *Crit. Rev. Toxicol. 25*, 397−462.

(6) Lee, T. C., Huang, R. Y., and Jan, K. Y. (1985) Sodium arsenite enhances the cytotoxicity, clastogenicity, and 6-thioguanine-resistant mutagenicity of ultraviolet light in Chinese hamster ovary cells. *Mutat. Res. 148*, 83−89.

(7) Lee, T. C., Oshimura, M., and Barrett, J. C. (1985) Comparison of arsenic-induced cell transformation, cytotoxicity, mutation and cytogenetic effects in Syrian hamster embryo cells in culture. *Carcinogenesis 6*, 1421−1426.

(8) Zhao, C. Q., Young, M. R., Diwan, B. A., Coogan, T. P., and Waalkes, M. P. (1997) Association of arsenic-induced malignant transformation with DNA hypomethylation and aberrant gene expression. *Proc. Natl. Acad. Sci. U.S.A. 94*, 10907−10912.

(9) Goering, P. L., Aposhian, H. V., Mass, M. J., Cebrian, M., Beck, B. D., and Waalkes, M. P. (1999) The enigma of arsenic carcinogenesis: Role of metabolism. *Toxicol. Sci. 49*, 5−14.

(10) Andrew, A. S., Karagas, M. R., and Hamilton, J. W. (2003) Decreased DNA repair gene expression among individuals exposed to arsenic in United States drinking water. *Int. J. Cancer 104*, 263−268.

(11) Abernathy, C. O., Liu, Y. P., Longfellow, D., Aposhian, H. V., Beck, B., Fowler, B., Goyer, R., Menzer, R., Rossman, T., Thompson, C., and Waalkes, M. (1999) Arsenic: health effects, mechanisms of actions, and research issues. *Environ. Health Perspect. 107*, 593−597.

(12) Liu, F., and Jan, K. Y. (2000) DNA damage in arsenite- and cadmium-treated bovine aortic endothelial cells. *Free Radical Biol. Med. 28*, 55−63.

(13) Lynn, S., Gurr, J. R., Lai, H. T., and Jan, K. Y. (2000) NADH oxidase activation is involved in arsenite-induced oxidative DNA damage in human vascular smooth muscle cells. *Circ. Res. 86*, 514−519.

(14) Ramirez, P., Del Razo, L. M., Gutierrez-Ruiz, M. C., and Gonsebatt, M. E. (2000) Arsenite induces DNA-protein cross-links and cytokeratin expression in the WRL-68 human hepatic cell line. *Carcinogenesis 21*, 701−706.

(15) Matsui, M., Nishigori, C., Toyokuni, S., Takada, J., Akaboshi, M., Ishikawa, M., Imamura, S., and Miyachi, Y. (1999) The role of oxidative DNA damage in human arsenic carcinogenesis: Detection of 8-hydroxy-2′-deoxyguanosine in arsenic-related Bowen's disease. *J. Invest. Dermatol. 113*, 26−31.

(16) Hei, T. K., Liu, S. X., and Waldren, C. (1998) Mutagenicity of arsenic in mammalian cells: role of reactive oxygen species. *Proc. Natl. Acad. Sci. U.S.A. 95*, 8103−8107.

(17) Iwama, K. (2001) Apoptosis induced by arsenic trioxide in leukemia U937 cells is dependent on activation of p38, inactivation of ERK and the Ca2+-dependent production of superoxide. *Int. J. Cancer 92*, 518−526.

(18) Liu, S. X., Athar, M., Lippai, I., Waldren, C., and Hei, T. K. (2001) Induction of oxyradicals by arsenic: implication for mechanism of genotoxicity. *Proc. Natl. Acad. Sci. U.S.A. 98*, 1643−1648.
(19) Barchowsky, A., Roussel, R. R., Klei, L. R., James, P. E., Ganju, N., Smith, K. R., and Dudek, E. J. (1999) Low levels of arsenic trioxide stimulate proliferative signals in primary vascular cells without activating stress effector pathways. *Toxicol. Appl. Pharmacol. 159*, 65−75.
(20) Corsini, E., Asti, L., Viviani, B., Marinovich, M., and Galli, C. L. (1999) Sodium arsenate induces overproduction of interleukin-1α in murine keratinocytes: Role of mitochondria. *J. Invest. Dermatol. 113*, 760−765.
(21) Jing, Y. (1999) Arsenic trioxide selectively induces acute promyelocytic leukemia cell apoptosis via a hydrogen peroxide-dependent pathway. *Blood 94*, 2102−2111.
(22) Cantoni, O. (1994) Cross-resistance to heavy metals in hydrogen peroxide-resistant CHO cell variants. *Mutat. Res. 324*, 1−6.
(23) Barchowsky, A., Klei, L. R., Dudek, E. J., Swartz, H. M., and James, P. E. (1999) Stimulation of reactive oxygen, but not reactive nitrogen species, in vascular endothelial cells exposed to low levels of arsenite. *Free Radical Biol. Med. 27*, 1405−1412.
(24) Tice, R. R., Andrews, P. W., Hirai, O., and Singh, N. P. (1991) The single cell gel (SCG) assay: An electrophoretic technique for the detection of DNA damage in individual cells. *Adv. Exp. Med. Biol. 283*, 157−164.
(25) Shi, X., Ding, M., Ye, J., Wang, S., Leonard, S. S., Zang, L., Castranova, V., Vallyathan, V., Chiu, A., Dalal, N., and Liu, K. (1999) Cr(IV) causes activation of nuclear transcription factor-κ B, DNA strand breaks and dG hydroxylation via free radical reactions. *J. Inorg. Biochem. 75*, 37−44.
(26) Shi, X., Leonard, S. S., Wang, S., and Ding, M. (2000) Antioxidant properties of pyrrolidine dithiocarbamate and its protection against Cr(VI)-induced DNA strand breakage. *Ann. Clin. Lab. Sci. 30*, 209−216.
(27) Shi, X., Mao, Y., Knapton, A. D., Ding, M., Rojanasakul, Y., Gannett, P. M., Dalal, N., and Liu, K. (1994) Reaction of Cr(VI) with ascorbate and hydrogen peroxide generates hydroxyl radicals and causes DNA damage: Role of a Cr(IV)-mediated Fenton-like reaction. *Carcinogenesis 15*, 2475−2478.
(28) Liu, K. J. H., Ye, J., Leonard, S. S., Cutler, D., Chen, F., Wang, S., Zhang, Z., Ding, M., Wang, L., and Shi, X. (2001) On the mechanism of Cr (VI)-induced carcinogenesis: Dose dependence of uptake and cellular responses. *Mol. Cell. Biochem. 222*, 221−229.
(29) Ding, M., and Shi, X. (2002) Molecular mechanisms of Cr(VI)-induced carcinogenesis. *Mol. Cell. Biochem. 234−235*, 293−300.
(30) Zhao, H., Kalivendi, S., Zhang, H., Joseph, J., Nithipatikom, K., Vasquez-Vivar, J., and Kalyanaraman, B. (2003) Superoxide reacts with hydroethidine but forms a fluorescent product that is distinctly different from ethidium: Potential implications in intracellular fluorescence detection of superoxide. *Free Radical Biol. Med. 34*, 1359−1368.
(31) Carter, W. O., Narayanan, P. K., and Robinson, J. P. (1994) Intracellular hydrogen peroxide and superoxide anion detection in endothelial cells. *J. Leukocyte Biol. 55*, 253−258.
(32) Bass, D. A., Parce, J. W., Dechatelet, L. R., Szejda, P., Seeds, M. C., and Thomas, M. (1983) Flow cytometric studies of oxidative product formation by neutrophils: A graded response to membrane stimulation. *J. Immunol. 130*, 1910−1917.
(33) Iwama, K., Nakajo, S., Aiuchi, T., and Nakaya, K. (2001) Apoptosis induced by arsenic trioxide in leukemia U937 cells is dependent on activation of p38, inactivation of ERK and the Ca2+-dependent production of superoxide. *Int. J. Cancer 92*, 518−526.
(34) Lynn, S. (2000) NADH oxidase activation is involved in arsenite-induced oxidative DNA damage in human vascular smooth muscle cells. *Circ. Res. 86*, 514−519.
(35) Pi, J., Qu, W., Reece, J. M., Kumagai, Y., and Waalkes, M. P. (2003) Transcription factor Nrf2 activation by inorganic arsenic in cultured keratinocytes: Involvement of hydrogen peroxide. *Exp. Cell. Res. 290*, 234−245.
(36) Jing, Y., Dai, J., Chalmers-Redman, R. M., Tatton, W. G., and Waxman, S. (1999) Arsenic trioxide selectively induces acute promyelocytic leukemia cell apoptosis via a hydrogen peroxide-dependent pathway. *Blood 94*, 2102−2111.
(37) Wang, T. S., Kuo, C. F., Jan, K. Y., and Huang, H. (1996) Arsenite induces apoptosis in Chinese hamster ovary cells by generation of reactive oxygen species. *J. Cell. Physiol. 169*, 256−268.
(38) Klaunig, J. E., and Kamendulis, L. M. (2004) The role of oxidative stress in carcinogenesis. *Annu. Rev. Pharmacol. Toxicol. 44*, 239−267.
(39) Rea, M. A., Gregg, J. P., Qin, Q., Phillips, M. A., and Rice, R. H. (2003) Global alteration of gene expression in human keratinocytes by inorganic arsenic. *Carcinogenesis 24*, 747−756.
(40) Boulikas, T. (1991) Relation between carcinogenesis, chromatin structure and poly(ADP-ribosylation) (review). *Anticancer Res. 11*, 489−527.
(41) Yih, L. H., and Lee, T. C. (2000) Arsenite induces p53 accumulation through an ATM-dependent pathway in human fibroblasts. *Cancer Res. 60*, 6346−6352.
(42) Wang, T. S., Hsu, T. Y., Chung, C. H., Wang, A. S., Bau, D. T., and Jan, K. Y. (2001) Arsenite induces oxidative DNA adducts and DNA-protein cross-links in mammalian cells. *Free Radical Biol. Med. 31*, 321−330.
(43) Shi, X. L., and Dalal, N. S. (1990) NADPH-dependent flavoenzymes catalyze one electron reduction of metal ions and molecular oxygen and generate hydroxyl radicals. *FEBS Lett. 276*, 189−191.
(44) Shi, X., Dalal, N. S., and Kasprzak, K. S. (1993) Generation of free radicals from hydrogen peroxide and lipid hydroperoxides in the presence of Cr(III). *Arch. Biochem. Biophys. 302*, 294−299.
(45) Shi, X., and Dalal, N. S. (1994) Generation of hydroxyl radical by chromate in biologically relevant systems: role of Cr(V) complexes versus tetraperoxochromate(V). *Environ. Health Perspect. 102* (Suppl. 3), 231−236.
(46) Yamanaka, K., Hoshino, M., Okamoto, M., Sawamura, R., Hasegawa, A., and Okada, S. (1990) Induction of DNA damage by dimethylarsine, a metabolite of inorganic arsenics, is for the major part likely due to its peroxyl radical. *Biochem. Biophys. Res. Comm. 168*, 58−64.
(47) Yamanaka, K., Hasegawa, A., Sawamura, R., and Okada, S. (1991) Cellular response to oxidative damage in lung induced by the administration of dimethylarsinic acid, a major metabolite of inorganic arsenics, in mice. *Toxicol. Appl. Pharmacol. 108*, 205−213.
(48) Yamanaka, K., and Okada, S. (1994) Induction of lung-specific DNA damage by metabolically methylated arsenics via the production of free radicals. *Environ. Health Perspect. 102* (Suppl. 3), 37−40.
(49) Ahmad, S., Kitchin, K. T., and Cullen, W. R. (2000) Arsenic species that cause release of iron from ferritin and generation of activated oxygen. *Arch. Biochem. Biophys. 382*, 195−202.
(50) Yamazaki, I. (1990) ESR spin-trapping studies on the reaction of Fe2+ ions with H2O2-reactive species in oxygen toxicity in biology. *J. Biol. Chem. 265*, 13589−13594.
(51) Del Razo, L. M., Styblo, M., Cullen, W. R., and Thomas, D. J. (2001) Determination of trivalent methylated arsenicals in biological matrixes. *Toxicol. Appl. Pharmacol. 174*, 282−293.
(52) Young, M. R., Li, J. J., Rincon, M., Flavell, R. A., Sathyanarayana, B. K., Hunziker, R., and Colburn, N. (1999) Transgenic mice demonstrate AP-1 (activator protein-1) transactivation is required for tumor promotion. *Proc. Natl. Acad. Sci. U.S.A. 96*, 9827−9832.

TX049939E